

Anomalous Buckling of Charged Rods

Roya Zandi,^{1,2} Ramin Golestanian,^{3,4} and Joseph Rudnick⁵

¹*Department of Chemistry and Biochemistry, UCLA, Box 951569, Los Angeles, CA 90095-1569*

²*Department of Physics, Massachusetts Institute of Technology, Cambridge, MA 02139, USA*

³*Institute for Advanced Studies in Basic Sciences, Zanjan 45195-159, Iran*

⁴*Institute for Studies in Theoretical Physics and Mathematics, P.O. Box 19395-5531, Tehran, Iran*

⁵*Department of Physics, UCLA, Box 951547, Los Angeles, CA 90095-1547*

(Dated: November 19, 2013)

Unscreened electrostatic interactions exert a profound effect on the onset of the buckling instability of a charged rod. When this interaction is unscreened, the threshold value of the compressional force needed to induce buckling is independent of rod length for sufficiently long rods. In the case of rods of intermediate length, the critical buckling force crosses over from the classic inverse-square length dependence to asymptotic length-independent form with increasing rod length. It is suggested that this effect might lead to the possibility of the “electromechanical” stiffening of nanotubes, which would allow relatively long segments of them to be used as atomic force probes.

PACS numbers: 46.32.+x, 82.35.Rs, 87.15.La, 85.35.Kt, 07.10.Cm

When slender objects are subjected to external compressional elastic forces, they are susceptible to bending deformations. The onset of such a deformation is known generically as the buckling instability [1, 7]. Mechanical failure also occurs in elastic and viscoelastic objects, such as falling ropes [2], “pouring” filaments of viscoelastic fluids [3] as they hit horizontal solid surfaces, and migrating geophysical fluids reaching their terminations [4]. An elastic rod of a given material and length can resist compressional forces up to a so-called *critical buckling force* F_c that increases with the (effective) bending stiffness of the rod, and decreases with an inverse-square law with its length L ($F_c \sim 1/L^2$). Because of this length dependence, longer filaments possess much lower critical buckling forces [1].

The limitation on rod length imposed by the buckling instability is a major structural issue in nano-scale mechanics (AFM-tips, nanotubes [5] and nanorods [6], etc.) as well as the micro- and macro-scale. However, this limitation results from the local nature of elasticity, and may in principle be overcome if long-ranged interactions also exert a stiffening influence. Here we study the mechanical response of an elastic charged rod to external compressional forces, and in particular the onset of Euler buckling instability, taking into account the nonlocal nature of electrostatic self-interactions. For a cylindrical charged rod of radius r and surface number charge density σ , we find that long-ranged electrostatics leads, in the limit of a long rod, to a non-vanishing critical buckling force

$$F_c(L \rightarrow \infty) = \Delta \frac{\pi}{\epsilon_0} e^2 \sigma^2 r^2, \quad (1)$$

in which ϵ_0 is the permittivity of free space, e is the electron charge, and $\Delta = 0.1137056$ is a universal numerical prefactor. In the case of rods with a finite length L , we find that the above result smoothly crosses over to a local $1/L^2$ dependence as L decreases. Crossover to this

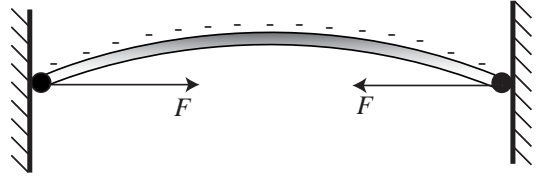


FIG. 1: The elastic charged rod is hinged at two ends and is subject to a compressional force F .

dependence occurs when L is small enough that the accumulated electrostatic self-interaction has not yet overwhelmed local elasticity. We also determine the shape of the rod at the onset of buckling, and show that the buckling rod becomes considerably flatter in the interior as a result of electrostatic self-repulsion.

The elastic charged rod is considered to be inextensible, and its energy consists of two contributions. The first part results from the elastic bending energy $E_b = \frac{K}{2} \int_0^L ds H(s)^2$. This energy is controlled by the intrinsic bending modulus K of the elastic rod and contains no electrostatic contributions. The curvature $H(s)$ is assumed to be a function of the arclength parameter s . For a homogeneous elastic rod of circular cross section that is made of a material with a Young’s modulus E , we have $K = \frac{\pi}{4} r^4 E$ [7].

The second contribution to the energy arises from electrostatic interactions, which can be written as $E_{el} = \frac{\Upsilon}{2} \int_0^L ds ds' \frac{1}{|\mathbf{r}(s) - \mathbf{r}(s')|}$, for a rod whose conformation is represented by a space curve $\mathbf{r}(s)$. The electrostatic coupling constant is defined as $\Upsilon = e^2 / (4\pi\epsilon_0 a^2)$, a being the average separation between neighboring charges along the line. Considering the cylindrical geometry of the rod, one can express the linear number charge density $1/a$ in terms of the surface number charge density σ through $a = (2\pi r \sigma)^{-1}$, which yields $\Upsilon = (\pi/\epsilon_0) e^2 \sigma^2 r^2$.

Finally, to study the onset of buckling upon apply-

ing a compressive force F , we add a term $E_{\text{ex}} = F \int_0^L ds \cos \theta(s)$ to the total energy.

One can estimate the critical buckling force for a neutral rod using a simple force balance argument. Imagine that the rod is bent into an arc of a circle of radius R with a corresponding arc angle θ , so that $L = R\theta$. Then we can calculate the bending energy $E_b(\theta) = \frac{KL}{2R^2} = \frac{K\theta^2}{2L}$, and the end-to-end distance $x(\theta) = 2R \sin \frac{\theta}{2} = L \sin \frac{\theta}{2} / (\frac{\theta}{2})$ as a function of the bending angle θ . The elastic force that resists bending at the onset of such arc formation can be found as $F_b = -\partial E_b(\theta) / \partial x(\theta)|_{\theta=0} = 12K/L^2$, which slightly overestimates the exact critical buckling force $F_{c0} = \pi^2 K/L^2$ [7] due to the artificial assumption of constant curvature. A similar argument can be used to qualitatively account for Eq. (1) in the case of a charged rod with negligible intrinsic rigidity. Imagine that charges of unit magnitude are placed along the rod in a regular pattern at a distance a from each other (see Fig. 1). The electrostatic repulsive force that the first charge experiences can then be calculated as the sum of the contributions from all the neighbors, namely, $F_{\text{el}}(1) = \Upsilon(1 + 1/2^2 + 1/3^2 + \dots) = \pi^2 \Upsilon/6$. If the charged rod is to undergo compressional failure, the external force has to be greater than this Coulomb repulsion, thus yielding the scaling form for the critical buckling force as reported in Eq. (1). To obtain the correct numerical prefactor, however, one should look collective failure corresponding to the lowest threshold critical force.

A convenient expansion of the total energy can be carried out in terms of a suitable deformation field. For the mechanical response that we would like to consider, it proves sufficient to focus only on planar deformations, which are conveniently characterized via the angle $\theta(s)$ that the rod's local unit tangent vector makes with its unperturbed orientation. Expanding the total energy up to second order then yields [8]

$$E_{\text{tot}} = \frac{K}{2} \int_0^L ds \left[\frac{d\theta(s)}{ds} \right]^2 - \frac{F}{2} \int_0^L ds \theta(s)^2 + \frac{\Upsilon}{2} \int_0^L ds ds' \mathcal{L}(s, s') \theta(s) \theta(s'), \quad (2)$$

where the electrostatic kernel is given as

$$\mathcal{L}(s, s') = \int_0^L ds_1 \int_{s_1}^L ds_2 \frac{1}{(s_2 - s_1)^3} \times \{ (s_2 - s_1) [\Theta(s - s_1) - \Theta(s - s_2)] \delta(s - s') - [\Theta(s - s_1) - \Theta(s - s_2)] [\Theta(s' - s_1) - \Theta(s' - s_2)] \}, \quad (3)$$

with $\Theta(s)$ the Heaviside step function. Note that $H(s) = d\theta(s)/ds$ in this representation.

The total energy is controlled by the spectrum of the following *total energy* bilinear operator

$$\mathcal{K}(F; s, s') = \left(-K \frac{d^2}{ds^2} - F \right) \delta(s - s') + \Upsilon \mathcal{L}(s, s'). \quad (4)$$

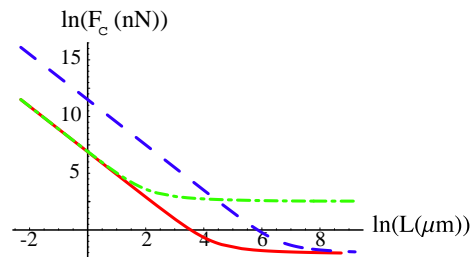


FIG. 2: The critical buckling force for a charged rod as a function of its length (log-log plot). (a) The solid line corresponds to $K = 1 \times 10^{-19} \text{ Nm}^2$ and $\Upsilon = 1 \text{ nN}$. (b) The dashed line corresponds to $K = 100 \times 10^{-19} \text{ Nm}^2$ and $\Upsilon = 1 \text{ nN}$. (c) The dash-dotted line corresponds to $K = 1 \times 10^{-19} \text{ Nm}^2$ and $\Upsilon = 100 \text{ nN}$.

While the eigenfunctions of this operator $\psi_n(s)$'s are the same as those for $\mathcal{K}(0; s, s')$, the eigenvalues have the form of $\mathcal{E}_n - F$, if \mathcal{E}_n 's are the eigenvalues of $\mathcal{K}(0; s, s')$. The onset of Euler instability is then found when the lowest eigenvalue $\mathcal{E}_0 - F$ passes through zero. For example, if we switch off electrostatics by setting $\Upsilon = 0$, the lowest eigenvalue will be $K\pi^2/L^2 - F$ that goes non-positive at the critical force $F_{c0} = \pi^2 K/L^2$. In Ref. [9], we have been able to calculate the exact spectrum of the electrostatic kernel $\mathcal{L}(s, s')$. The eigenvalues are found to be [10]

$$\lambda_k = \frac{1}{2} \left[2\gamma + \psi\left(\frac{1}{2} + ik\right) + \psi\left(\frac{1}{2} - ik\right) + \frac{3 - 4k^2}{1 + 4k^2} \right], \quad (5)$$

where $\gamma = 0.577216$ is the Euler constant, and $\psi(x) = d \ln \Gamma(x) / dx$ is the digamma function. Using this exact result, we can determine the critical buckling force for an infinitely long charge rod (or equivalently a charged rod with negligible intrinsic stiffness) as reported in Eq. (1) above, in which the numerical prefactor is calculated as $\Delta \equiv \lambda_0 = \gamma + \psi(1/2) + 3/2 \simeq 0.1137056$. The existence of a non-zero critical force in this limit is a manifestation of the long-ranged nature of electrostatic interactions.

Exactly at the onset of instability, the lowest eigenfunction (the ground state) $\psi_0(s)$ has a vanishing eigenvalue, and thus provides a nonzero solution to the homogeneous Euler-Lagrange equation corresponding to Eq. (2). With the appropriate boundary conditions, this solution provides the shape of the elastic charged rod at the onset of instability. We use a cosine basis expansion for the eigenfunction as $\psi_0(s) = \sum_{n=1} A_n \cos\left(\frac{n\pi s}{L}\right)$ that corresponds to the boundary condition of a rod with two hinged ends. The shape of the deformed rod can be found as

$$u(s) = \int_0^s ds' \psi_0(s') = L \sum_{n=1} \frac{A_n}{n\pi} \sin\left(\frac{n\pi s}{L}\right). \quad (6)$$

Note that in the absence of electrostatics we have $u_0(s) = c_0 \sin\left(\frac{\pi s}{L}\right)$ [7].

We study the spectrum of the total energy operator $\mathcal{K}(0; s, s')$ numerically [11], and use it to find the critical

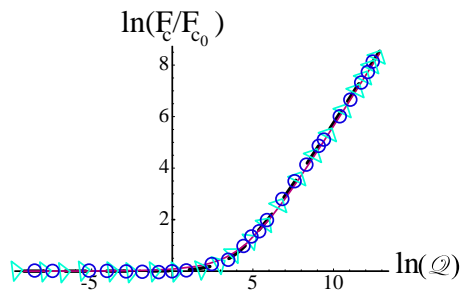


FIG. 3: The rescaled critical buckling force for a charged rod as a function of the charging parameter $\mathcal{Q} = \Upsilon L^2/K$. Note that three distinct series of data (hollow circles, triangles, and dashed line), corresponding to the different curves in Fig. 2, have been collapsed on top of a universal curve. The solid line represents the interpolation formula of Eq. (7) for comparison.

buckling force and the shape of a charged rod of arbitrary length at the onset of compressive failure. In Fig. 2, the critical buckling force is plotted as a function of the length of the rod, for various values of K and Υ . The plot shows an small- L $1/L^2$ dependence for the critical force that crosses over to an L -independent saturation value as L passes through a crossover length scale ℓ_x , where $\ell_x \propto \sqrt{K/\Upsilon}$.

The critical buckling forces corresponding to different values of the parameters K , Υ , and L can be collapsed onto a universal curve as shown in Fig. 3, if normalized with the critical buckling force of the neutral chain F_{c0} and plotted as a function of the dimensionless *charging parameter* $\mathcal{Q} = \Upsilon L^2/K$. An interpolation formula of the form

$$\frac{F_c}{F_{c0}} = 1 + \frac{1}{\pi^2} \sqrt{\frac{\mathcal{Q}}{2}} + \frac{\Delta}{\pi^2} \mathcal{Q}, \quad (7)$$

is found to satisfactorily represent the universal curve as revealed by the comparison in Fig. 3.

The shape of the charged rod at the onset of buckling is also calculated, and shown in Fig. 4 for various values of the charging parameter \mathcal{Q} . It appears that charging leads to deviations in the shape of the buckling rod from the sinus-profile [7] in that there is enhanced flattening in the interior. This is to be expected because the interior of the charged rod is subject to stronger build-up of electrostatic self-repulsion as compared to the end-segments where “half” of the repelling charges are absent. A similar effect has also been observed in the bending response of charged elastic rods [12].

We can also study the buckling instability for charged rodlike polymers, or polyelectrolytes, in a solution by using the screened Debye-Hückel interaction $e^{-\kappa r}/(\epsilon r)$ instead of the long-ranged Coulomb $1/r$ interaction, where ϵ is the zero-frequency dielectric constant of the solution and κ^{-1} represents the Debye screening length. The

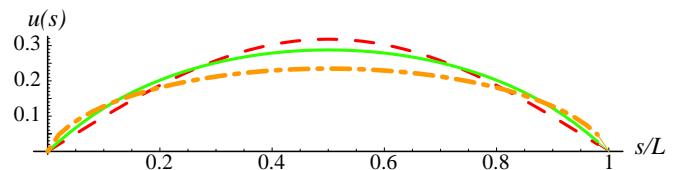


FIG. 4: The shape of a charged rod at the onset of Euler buckling instability. The dashed line corresponds to $\mathcal{Q} = 0$, the solid line corresponds to $\mathcal{Q} = 10^3$, and the dash-dotted line corresponds to $\mathcal{Q} = 10^6$. The buckling charged rod flattens in the interior as the charging is increased.

eigenvalues of the total energy can be calculated numerically for the screened case, and can be used to determine F_c for each set of parameters. We find that for sufficiently long polyelectrolytes the critical buckling force is given as $F_c = \pi^2 k_B T (\ell_0 + \ell_{\text{OSF}})/L^2$, in which $\ell_0 = K/k_B T$ is the intrinsic persistence length, and $\ell_{\text{OSF}} = \Upsilon/(4\epsilon k_B T \kappa^2)$ is the well-known Odijk-Skolnick-Fixman electrostatic persistence length for polyelectrolytes [8, 13]. This result confirms that the so-called wormlike chain description of polyelectrolytes remains valid in determining their mechanical response and onset of buckling instability, as long as $\kappa L \gg 1$ [9, 14]. For shorter chains, however, the $1/L^2$ dependence is altered, and a crossover similar to the one described in Fig. 2 takes place. As a particular case of interest for assessing the wormlike chain model of polyelectrolytes one can consider the unscreened limit ($\kappa = 0$), where it predicts a crossover of the form $F_c = \frac{\pi^2 K}{L^2} + \frac{\pi^2 \Upsilon}{72} = F_{c0} \left(1 + \frac{0.137078}{\pi^2} \mathcal{Q}\right)$ [8], which is to be contrasted with Eq. (7) above.

The familiar image of a long-haired girl touching the van de Graaff machine suggests that a practical way of imposing the required charging is by applying a voltage. For a conducting cylinder of length L and radius r that is kept at a potential V relative to “infinity” [15], one can calculate the induced surface charge density, and deduce from it the corresponding asymptotic critical buckling force as

$$F_c(L \rightarrow \infty, V) = \frac{\Delta \pi \epsilon_0 V^2}{[\ln(L/r)]^2}. \quad (8)$$

For a thread of human hair we have $r \simeq 0.1$ mm and $K_{\text{hair}} \sim 10^{-11}$ Nm², which yields for $L = 1$ cm a critical force of $F_c \simeq 10^{-6}$ N. Applying a voltage of $V = 50$ kV (typical of van de Graaff generators) then results in a critical force of $F_c \simeq 10^{-4}$ N for a one-meter long piece of hair!

Perhaps the most interesting venue in which these results find application will be in hardening of atomic force probes. Carbon nanotubes have been found to be structurally quite robust and have exceptionally high Young’s modulus (in the TPa range) [16]. However, the fact that they can grow up to microns in length while having nanometric diameters renders them quite susceptible to

buckling. The buckling of multi-walled carbon nanotubes have been recently investigated experimentally by Dong *et al.* [17]. In their experiment, a 6.9 μm long nanotube have been placed under compression and its critical buckling force (typically in the nN range for micron-sized nanotubes) have been measured, from which they could extract the bending rigidity of the nanotube as $K_{\text{nanotube}} = 8.641 \times 10^{-20} \text{ Nm}^2$ [17]. Using Eq. (8), we can now estimate that a carbon nanotube 30 nm in diameter can resist forces up to ~ 1 nN even when it is 1 mm long, provided it is kept at a voltage of 200 V. This implies a remarkable “electromechanical stiffness,” in contrast with the intrinsic mechanical resistance to buckling which is diminished by a factor of 10^6 when the length of the nanotube is increased from a micron to a millimeter. The stiffening mechanism may also be useful in the recently reported nanometer-scale electromechanical actuator that is based on a multi-walled carbon nanotube [18].

The authors would like to acknowledge helpful discussions with D. Chatenay, L. Dong, and T.B. Liverpool. RZ acknowledges support from the UC President’s Postdoctoral Fellowship program. This research was supported by the National Science Foundation under Grant No. CHE99-88651.

-
- [1] A.E.H. Love, *A Treatise on the Mathematical Theory of Elasticity*, 2nd edition (Dover, London, 1944).
 [2] L. Mahadevan and J.B. Keller, Proc. R. Soc. Lond. A **452**, 1679 (1996).
 [3] L. Mahadevan, W.S. Ryu, and A.D. Samuel, Nature **392**, 140 (1998); Erratum: L. Mahadevan, W.S. Ryu, and A.D. Samuel, Nature **403**, 502 (2000).

- [4] A.M. Johnson and R.C. Fletcher, *Folding of Viscous Layers* (Columbia, New York, 1994).
 [5] B.I. Yakobson, C.J. Brabec, and J. Bernholc, Phys. Rev. Lett. **76**, 2511 (1996).
 [6] E.W. Wong, P.E. Sheehan, and C.M. Lieber, Science **277**, 1971 (1997).
 [7] L.D. Landau and E.M. Lifshitz, *Theory of Elasticity*, 3rd edition (Butterworth-Heinemann, Oxford, 1986).
 [8] T. Odijk, J. Polym. Sci. **15**, 477 (1977).
 [9] R. Zandi, J. Rudnick, and R. Golestanian, Phys. Rev. E **67**, 021803 (2003).
 [10] We are correcting here a missing factor of $\frac{1}{2}$ in the results reported in Ref. [9] [required in Eqs. (B12) and (B15) therein].
 [11] The details of the numerical method is explained in Ref. [9].
 [12] R. Zandi, J. Rudnick, and R. Golestanian, Phys. Rev. E **67**, 061805 (2003).
 [13] J. Skolnick and M. Fixman, Macromolecules **10**, 944 (1977).
 [14] R. Zandi, J. Rudnick, and R. Golestanian, Eur. Phys. J. E **9**, 41 (2002).
 [15] If a conducting rod is held at a constant electrostatic potential, the charge distribution along the rod is known to be nearly uniform. The slight logarithmic buildup of charge at the ends of the rod leads to no significant change in the electrostatic energetics of the buckled rod; the conclusions reported in the body [Eq. (8) and the related discussions] are not materially affected.
 [16] M.M.J. Treacy, T.W. Ebbesen, and J.M. Gibson, Nature **381**, 678 (1996).
 [17] L. Dong, F. Arai, and T. Fukuda, Proceedings of the 2001 IEEE International Conference on Robotics & Automation (Seoul, Korea, May 21-26, 2001); J. of Robotics and Mechatronics **14**, 245 (2002).
 [18] A.M. Fennimore, T.D. Yuzvinsky, W.Q. Han, M.S. Fuhrer, J. Cumings, and A. Zettl, Nature **424**, 408 (2003).